

# Exploring the Anti-Seborrheic Dermatitis Potential of *Prunus armeniaca* L. Seed Oil: A Stereological, Biochemical and Molecular Study on MMP-9, MMP-2, CCR-5 and VEGF Pathways in a Rat Model

Explorando el Potencial del Aceite de Semilla de *Prunus armeniaca* l. para la Dermatitis Seborreica: Un Estudio Estereológico, Bioquímico y Molecular Sobre las Vías de MMP-9, MMP-2, CCR-5 y VEGF en un Modelo de Rata

Nan Ren<sup>1</sup> & Rongrong Tan<sup>1</sup>

**REN, N. & TAN, R.** Exploring the anti -seborrheic dermatitis potential of *Prunus armeniaca* L. seed oil: A stereological, biochemical and molecular study on MMP-9, MMP-2, CCR-5, and VEGF pathways in a rat model. *Int. J. Morphol.*, 43(6):2070-2078, 2025.

**SUMMARY:** *Prunus armeniaca* L. Seed Oil (PASO) has been historically utilized for its medicinal benefits, including enhancing vitality and managing bleeding. Its traditional applications are backed by its antibacterial, anti-inflammatory, and anti-seborrheic properties. This study aimed to explore the mechanisms behind PASO's anti-inflammatory and anti-seborrheic effects, particularly in relation to hair regrowth and seborrheic dermatitis (SD), by assessing its capacity to lower sebum production and prevent hair loss. The research involved 50 Wistar rats, divided into five groups (n=10 each): a sham group, a group exposed to 0.8 % dinitrofluorobenzene (DNFB) at 2 mg/kg, two DNFB group treated with 50 and 100 mg/kg PASO, and a sham group treated with 100 mg/kg PASO. At the conclusion of the study, we evaluated skin tissue for levels of critical inflammatory cytokines (IL-1 $\beta$ , IL-10, and TNF- $\alpha$ ) and oxidative stress indicators, including total antioxidant capacity and lipid peroxidation. Additionally, we assessed the expression of genes and proteins such as MMP-9, MMP-2, CCR-5, and VEGF in the skin tissue. Our results indicated that DNFB treatment led to significant changes in antioxidant levels, inflammatory markers, and the expression of genes and proteins associated with SD. Treatment with PASO demonstrated a dose-dependent improvement, particularly at 10 mg/kg, effectively reversing these alterations. Histopathological and molecular analyses confirmed the structural restoration of skin tissue following PASO treatment. In conclusion, this study underscores the potential of PASO in alleviating symptoms of seborrheic dermatitis and regulating skin inflammation, suggesting its potential application in managing DNFB-induced SD.

**KEY WORDS:** Virgin coconut oil; Inflammation; Apoptosis; Anti-seborrheic.

## INTRODUCTION

Seborrheic dermatitis (SD) is a chronic inflammatory skin disorder that primarily affects regions with a high concentration of sebaceous glands, including the scalp, face, eyebrows, and chest. It is estimated to affect around 3-10 % of the global population, with a higher incidence noted in males and among individuals with neurological conditions or weakened immune systems (Jackson *et al.*, 2024). Clinically, SD presents as flaky, inflamed, and red skin, often accompanied by itching. The onset of this condition is influenced by multiple factors, including genetic susceptibility, hormonal changes, stress, and the presence of *Malassezia* yeasts—lipophilic fungi that metabolize skin lipids and incite inflammatory responses (Li *et al.*, 2022). Recent research emphasizes the significant role of *Malassezia* in the pathogenesis of SD; its enzymes and

metabolites can trigger inflammation, which is exacerbated by an imbalance between pro-inflammatory and anti-inflammatory cytokines, particularly those involving Th1 and Th17 cell subsets. Furthermore, SD is linked to a compromised skin barrier, making it more vulnerable to irritants and environmental factors (Xian *et al.*, 2025). New therapeutic strategies are focusing on specific cytokines such as IL-17 and IL-23, as well as innovative topical treatments designed to alleviate inflammation and restore skin barrier function. Additionally, probiotic and prebiotic approaches are being explored for their potential to modulate skin microbiota (Wan, 2023). Future studies aim to enhance our understanding of the skin microbiome's role and to develop personalized treatment options to improve management, particularly for severe or recurrent cases. The epidemiology

<sup>1</sup> Department of Dermatology and Plastic Cosmetic Surgery, Xi'an Daxing Hospital, Xi'an City, Shaanxi Province 710003, China.

of SD exhibits a distinct pattern, with peak occurrences during infancy and adolescence—key periods characterized by hormonal shifts and heightened sebaceous gland activity. This condition often persists into adulthood as a relapsing issue, frequently aggravated by environmental and emotional stressors (Polaskey *et al.*, 2024). Males are disproportionately affected, likely due to the androgenic stimulation of sebaceous glands and the modulation of immune responses. Additionally, there are notable associations with neurological disorders such as Parkinson's disease and immune suppression conditions like HIV, highlighting the complex relationship between immune status and susceptibility to the disease (Hill *et al.*, 2025).

The pathogenesis of SD involves a complex interplay of microbial, genetic, and immune factors, with the colonization of *Malassezia* spp. being central. These fungi produce enzymes that incite inflammation and lipid metabolites that irritate the skin. Their overgrowth is facilitated by increased sebum production—stimulated by androgens—and compromised skin barrier function, which together promote fungal proliferation and immune activation (Sowell *et al.*, 2022). Recent research has also underscored the importance of oxidative stress; an imbalance that favors reactive oxygen species (ROS) leads to cellular damage, lipid peroxidation (e.g., elevated levels of malondialdehyde), and a reduction in antioxidant defenses like superoxide dismutase, catalase, and glutathione peroxidase (Li *et al.*, 2025). These oxidative stress processes activate critical transcription factors such as NF- $\kappa$ B and AP-1, which drive pro-inflammatory cytokine cascades and perpetuate inflammation. At the molecular level, the upregulation of matrix metalloproteinases (MMP-2 and MMP-9) facilitates tissue remodeling and undermines skin barrier integrity, while the heightened expression of the chemokine receptor CCR-5 promotes immune cell infiltration, further sustaining inflammation (Fernández *et al.*, 2022). Additionally, increased levels of vascular endothelial growth factor (VEGF) contribute to angiogenesis and skin hypervascularity, exacerbating lesion severity (Kapoor *et al.*, 2023). Collectively, these findings illustrate that the pathogenic landscape of SD involves a multifaceted interaction of pro-inflammatory cytokines, oxidative stress, and molecular pathways that drive tissue degradation and immune activation, representing potential targets for therapeutic intervention.

*Prunus armeniaca* L. Seed Oil (PASO) is derived from the mature seeds of the *Prunus armeniaca*, a tropical plant widely cultivated in areas such as Southeast Asia, the Pacific Islands, India, the Philippines, and the Caribbean. This member of the Rosaceae family flourishes in sunny, coastal environments. The extraction of PASO typically

employs cold-pressing or wet-milling techniques, which help retain its natural bioactive compounds, ensuring both high purity and nutritional value (Aleksanyan *et al.*, 2024). Recent investigations have validated many of these traditional applications, showcasing PASO's extensive pharmacological advantages, including antimicrobial and antiviral effects—primarily attributed to medium-chain fatty acids such as lauric, caprylic, and capric acids. Furthermore, it exhibits anti-inflammatory, antioxidant, cardiovascular, and neuroprotective properties, which enhance lipid profiles, mitigate oxidative stress, and provide alternative energy sources for brain cells (Alajil *et al.*, 2021). Nutritionally, PASO is abundant in vitamins E and K, as well as beta-carotene precursors and essential minerals like magnesium, calcium, iron, and phosphorus. Its polyphenolic compounds—including phenolic acids, flavonoids, and tocotrienols—further amplify its antioxidant, anti-inflammatory, and antimicrobial capabilities (Cirillo *et al.*, 2023). Cellular and molecular research supports these findings, demonstrating PASO's efficacy in neutralizing reactive oxygen species, inhibiting NF- $\kappa$ B-mediated inflammatory pathways—which lowers cytokines such as IL-1 $\beta$ , IL-6, and TNF- $\alpha$ —and disrupting microbial cell membranes through lauric acid, thereby diminishing pathogen proliferation (Konar *et al.*, 2020). Additionally, it promotes tissue regeneration by activating dermal repair mechanisms and bolstering skin barrier integrity, positioning it as an effective natural agent for managing various skin disorders (Alajil *et al.*, 2021). In this study, we investigated the antiseborrheic effects of PASO using an animal model of SD, focusing on its influence on inflammatory and antioxidant pathways, as well as its potential in repairing skin damage induced by dinitrofluorobenzene (DNFB).

## MATERIAL AND METHOD

**Preparation of PASO.** A total of 1800 g of PASO juice and melt were meticulously blended in equal proportions with a 50:50 (v/v) mixture of ethanol and acetone, then incubated at 37 °C for 48 hours. After this incubation period, the mixture was filtered and stored in the dark at room temperature for an additional 48 hours. The sample was then filtered through filter paper and concentrated using a rotary evaporator. After 48 hours of fermentation, two distinct layers emerged; the upper layer, which contained the oil, was collected after being refrigerated. This oil was separated through centrifugation at 12000 rpm for 12 minutes and subsequently filtered to yield a pure oily layer. The final ointment, weighing 400 g, was stored at 4 °C. An allergy test was conducted on five rats, with a screening duration of 48 hours under controlled conditions (Wang *et al.*, 2021).

## Experimental design, SD model, and animal grouping

Following a one-week acclimatization phase, rats weighing approximately  $220\pm8$  g were randomly divided into five groups, each consisting of ten animals. The rats were housed in propylene cages, maintained under a 12-hour light/dark cycle at a temperature of  $26\pm3$  °C and a humidity level of  $36\pm5$  %. They had access to tap water and a standard pellet diet. To induce seborrheic dermatitis, a 50  $\mu$ l application of a 0.8 % (4 mg/kg) DNFB (Sigma, USA) ointment—formulated with 50 % olive oil, 25 % acetone, and 18 % DMSO (v/v/v)—was applied to the inner surfaces of both ears and the shaved inguinal regions on day 1. On day 30, skin-fold thickness at these sites was measured using a micrometer, both immediately before the challenge and at 6 and 12 hours' post-application, with any increase indicating inflammatory swelling. For ease of handling, the rats were sedated with isoflurane. The sham group received a topical application of 0.2 ml of PBS, while the seborrheic dermatitis (SD) group was treated with the 0.8 % DNFB ointment. In the treatment groups, the SD rats received topical applications of PASO ointment at doses of either 50 or 100 mg/kg. Additionally, the sham+100 PASO group received 100 mg/kg of PASO ointment topically. This study aimed to identify an effective, non-toxic dose of PASO through daily topical administration at 9 a.m. over a period of 45 days, informed by preliminary data and prior research involving collagenase and PASO. All animal care and euthanasia procedures adhered to the ethical guidelines established by the Daxing Hospital, Xi'an City, Shaanxi Province ethics committee, in compliance with established laboratory animal welfare standards (Li *et al.*, 2025; Saleem *et al.*, 2022).

## Analysis of Antioxidant Levels and Lipid Peroxidation in Dermal Samples

To evaluate thiol concentrations in skin tissue, which serve as a key indicator of antioxidant status, 100  $\mu$ l of the skin homogenate was combined with 20  $\mu$ l of 5,5'-dithiobis (2-nitrobenzoic acid) (DTNB). The mixture was incubated at 37 °C for 15 min, followed by centrifugation at 12,000 g for 5 min. The absorbance of the supernatant was then measured at 412 nm using an ELISA plate reader (Bawadood *et al.*, 2024).

For the determination of lipid peroxidation (LPO) levels, the Thiobarbituric Acid Reactive Substances (TBARS) assay was employed. An aliquot of 100  $\mu$ l from the skin tissue homogenate was placed in a 2 ml polyethylene tube, followed by the addition of 100  $\mu$ l of TBARS reagent. The mixture was incubated at 37 °C for 30 min to facilitate the reaction. The absorbance was then measured at 593 nm to quantify LPO levels (Ertekin & Keçeci, 2022).

The total antioxidant capacity (TAC) of skin tissue was evaluated using the Ferric-Reducing Antioxidant Power (FRAP) assay. Skin samples were collected from the peri-ovarian fat and thoroughly homogenized. From each homogenate, 100  $\mu$ l was combined with 200  $\mu$ l of cold phosphate-buffered saline (PBS) in a 2 ml polyethylene tube. To this mixture, 10  $\mu$ l of the FRAP reagent was added, and the samples were incubated at 25 °C for 15 min. Following incubation, the samples were centrifuged at 12,000 g for 10 min, and the absorbance of the supernatant was measured at 593 nm (Bawadood *et al.*, 2024).

## Evaluation of Gene Expression Profiles: VEGF, CCR-5, IL-10, MMP-2, TNF- $\alpha$ , MMP-9, and IL-1 $\beta$ in skin tissue

Total RNA was isolated using TRIzol Reagent (Invitrogen) according to the manufacturer's instructions. The integrity of the isolated RNA was confirmed by running a 1 % agarose gel, while its purity and concentration were assessed using a NanoDrop spectrophotometer (Bio-TeK, USA). Subsequently, 2000 ng of the purified RNA underwent reverse transcription into cDNA using the RevertAid First Strand cDNA Synthesis Kit (Thermo Fisher Scientific), following the provided protocol. The synthesized cDNA was stored at -20 °C until further use. Quantitative real-time PCR was performed with SYBR Green (Vazyme, China) on an ABI 7900 fluorescence PCR system (ABI, USA). The PCR protocol included an initial step at 50 °C for 2 min, followed by denaturation at 95 °C for 10 min, and then 40 amplification cycles consisting of 30 s at 95 °C and 30 s at 60 °C. Primer sequences used in the study are listed in Table I. Gene expression levels were normalized to  $\beta$ -actin, and relative quantification was calculated using the Ct method, applying the  $\Delta\Delta Ct$  calculation and the corresponding fold change formula.

$2^{-\Delta\Delta Ct}$ ;  $\Delta\Delta Ct = [(Ct \text{ sample} - Ct \beta\text{-actin gene}) - (Ct \text{ sample} - Ct \text{ control})]$  (Amirouche *et al.*, 2021).

Table I. Primer sequences

Gene	Sequences (5'-3')
IL-1 $\beta$	F: GCAACTGTTCTGAACTCAACT
VEGF	F: TGCAGATTATCGGGATCAAACC
CCR-5	F: GATGGTGGTCTTCCTGCTGT
MMP-9	F: TGGACCGCTATGGTACA CC
TNF- $\alpha$	F: CCCACGTAGCAAAACCACCAA
MMP-2	F: GATAACCTGGATGCCGTGTT
$\beta$ -actin	F: TGAAGGTCGGAGTCAACGG

## Evaluation of MMP-9, MMP-2, CCR-5, and VEGF protein levels in skin tissue using western blotting

Specimens were lysed using RIPA buffer supplemented with phosphatase and protease inhibitors for

30 min. Protein levels were quantified using a BCA protein assay kit from Beyotime (China). For protein isolation, 40 mg of total protein was loaded onto a 10 % SDS-polyacrylamide gel for electrophoresis, followed by transfer to a PVDF membrane. The membranes were blocked with a 5 % (w/v) skim milk powder solution for 1 h. Subsequently, the membranes were incubated overnight at 4 °C with the following primary antibodies: anti-VEGF (Cat. No. ab51745; dilution 1:500), anti-MMP-2 (Cat. No. ab97779; dilution 1:400), anti-CCR-5 (Cat. No. ab287959; dilution 1:500), and anti-MMP-9 (Cat. No. ab38898; dilution 1:400), all obtained from Abcam (UK). After washing the membranes three times with PBST, they were incubated with an HRP-conjugated secondary antibody (dilution 1:5000) for 1 h. Band visualization was achieved using Bio-Rad's Stain-Free Gels, and the intensity of the bands was quantified using ImageJ gel analysis software (Kassassir *et al.*, 2023).

### Stereological assesments of skin layers

Rats were anesthetized with an intraperitoneal injection of 0.5 ml diazepam (50 mg/ml), after which skin tissues were carefully excised and fixed in 10 % formalin. The tissues were then embedded in paraffin and sectioned into 5 mm thick slices using a microtome (Model No. SM2010RV1.2, LEICA, Germany). The sections underwent deparaffinization and rehydration through an ethanol gradient, followed by hematoxylin and eosin (H&E) staining for histological examination. Additionally, Mallory Trichrome staining was performed to differentiate muscle from collagen fibers; skin tissue was fixed in Bouin's solution for at least 24 h, rinsed with running tap water, dehydrated through a graded ethanol series (70 %, 95 %, and 100 % ethanol), and cleared in xylene before embedding in paraffin wax. Sections were cut at 4-6  $\mu$ m thickness, deparaffinized in xylene for 2-3 min, and rehydrated through a graded ethanol series (100 %, 95 %, and 70 %) for 2-3 min each. They were then stained with Weigert's Iron Hematoxylin solution for 10 min, followed by Acid Fuchsin for 2-5 min, rinsed in distilled water, differentiated in Phosphomolybdic acid solution for 5-10 min, and stained with Aniline Blue for 5-10 min before being mounted on glass slides and dried. Histological analysis was conducted using a light microscope at  $\times 400$  magnification, with images captured using a BX61TRF light microscope system (Olympus, Japan) and analyzed with ImageJ software. Average thickness measurements of various skin layers and structures, including the epidermal (both stratum corneum and cellular layers), dermal, and hypodermal layers, were obtained using a BX61TRF light microscope fitted with a KEcam (KEcam Technologies, Nigeria) and Top View software (Version 3.7) (Fig. 1).

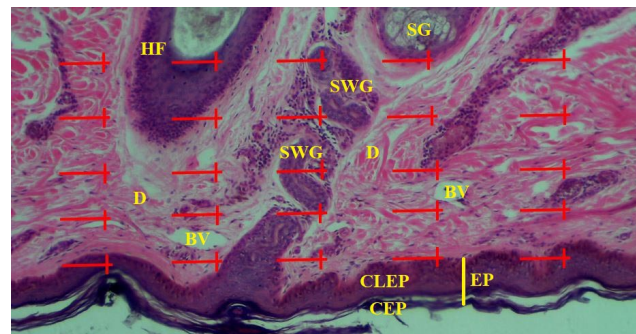


Fig. 1. Line probe (25 lines) used to estimate the surface density of skin structures. The total number of lines intersecting each structure ( $\Sigma p$ ), the length of each line in the probe determined by linear magnification ( $l/p$ ), and the number of lines intersecting the internal parts of the structures (SI) are recorded. The density calculation is performed using the formula:  $Sv=2\bar{Y} SI/\Sigma p \times l/p$  (H&E staining,  $\times 40$ ; Scale bar: 100  $\mu$ m). The accompanying light photomicrograph displays the skin, with labels indicating the epidermis layer (EP), dermis layer (D), corneal epidermis (CEP), cellular epidermis (CLEP), hair follicle (HF), sebaceous gland (SG), sweat gland (SWG), and blood vessels (BV).

### Statistical analyses

Data analysis was performed using SPSS version 16. The normality of the data was assessed with the Kolmogorov-Smirnov test. Results are presented as mean  $\pm$  standard deviation (SD). One-way analysis of variance (ANOVA) was employed to analyze the data. A P-value of less than 0.05 was considered statistically significant.

## RESULTS

### Role of PASO and SD on stereological assessments of skin layers

The SD group exhibited markedly reduced densities of sweat glands ( $0.161 \pm 0.09$  vs.  $0.321 \pm 0.11$   $\text{mm}^2$ ), sebaceous glands ( $0.141 \pm 0.05$  vs.  $0.329 \pm 0.11$   $\text{mm}^2$ ), and hair follicles ( $0.26 \pm 0.08$  vs.  $0.51 \pm 0.06$   $\text{mm}^2$ ) compared to the Sham group ( $p < 0.05$ ). Supplementation with 50 mg/kg and 100 mg/kg PASO significantly improved these parameters: the SD + 100 PASO group demonstrated near-normalization of sweat gland density ( $0.311 \pm 0.07$   $\text{mm}^2$ ), sebaceous gland density ( $0.294 \pm 0.09$   $\text{mm}^2$ ), and hair follicle density ( $0.55 \pm 0.09$   $\text{mm}^2$ ), all significantly higher than the SD group ( $p < 0.05$ ). Blood vessel density also increased in the SD + 100 PASO group ( $0.36 \pm 0.08$  vs.  $0.21 \pm 0.04$   $\text{mm}^2$  in SD;  $p < 0.05$ ), while interstitial structures showed partial recovery ( $0.22 \pm 0.06$  vs  $0.41 \pm 0.05$   $\text{mm}^2$  in SD;  $p < 0.05$ ) (Table II).

The SD group displayed abnormal epidermal thickness, with reduced cellular epidermal thickness ( $8.2 \pm$

Table II. Density measurements (in  $\text{mm}^2$ ) of sebaceous glands, sweat glands, hair follicles, blood vessels, and interstitial structures in the skin were assessed based on surface density (SV) and reference volume.

Groups	Sweat gland	Interstitial structures	Sebaceous gland	Blood vessels	Hair follicle
Sham	0.321 $\pm$ 0.11	0.16 $\pm$ 0.04	0.329 $\pm$ 0.11	0.42 $\pm$ 0.09	0.51 $\pm$ 0.06
SD	0.161 $\pm$ 0.09 <sup>a</sup>	0.41 $\pm$ 0.05 <sup>a</sup>	0.141 $\pm$ 0.05 <sup>a</sup>	0.21 $\pm$ 0.04 <sup>a</sup>	0.26 $\pm$ 0.08 <sup>a</sup>
Sham + 100 PASO	0.241 $\pm$ 0.14	0.21 $\pm$ 0.05	0.411 $\pm$ 0.10	0.39 $\pm$ 0.03	0.59 $\pm$ 0.06
SD + 50 PASO	0.189 $\pm$ 0.05	0.34 $\pm$ 0.09	0.169 $\pm$ 0.08 <sup>b</sup>	0.29 $\pm$ 0.07	0.42 $\pm$ 0.08 <sup>b</sup>
SD + 100 PASO	0.311 $\pm$ 0.07 <sup>b</sup>	0.22 $\pm$ 0.06 <sup>b</sup>	0.294 $\pm$ 0.09 <sup>b</sup>	0.36 $\pm$ 0.08	0.55 $\pm$ 0.09 <sup>b</sup>

Data are presented as mean  $\pm$  standard deviation (SD). <sup>a</sup> $p < 0.05$  indicates a significant difference between the sham and SD groups; <sup>b</sup> $p < 0.05$  indicates significant differences among the SD + 50 PASO and SD + 100 PASO groups compared to the SD groups (one-way ANOVA with Tukey's post-hoc test).

1.2 vs 21.3  $\pm$  1.6 mm in Sham) and elevated corneal epidermal thickness (11.1  $\pm$  0.9 vs. 2.9  $\pm$  0.2 mm in Sham;  $p < 0.05$ ). PASO supplementation reversed these effects: the

SD + 100 PASO group restored cellular epidermal thickness to Sham-like levels (20.6  $\pm$  2.2 mm;  $p < 0.05$  vs. SD) and reduced corneal thickness to 3.4  $\pm$  0.9 mm ( $p < 0.05$  vs. SD).

Total skin thickness increased by 65 % in the SD + 100 PASO group (349.7  $\pm$  16.1 vs. 211.2  $\pm$  18.4 mm in SD;  $p < 0.05$ ), while the SD + 50 PASO group showed moderate improvements in cellular epidermal thickness (12.6  $\pm$  1.1 mm;  $p < 0.05$  vs. SD) but no significant changes in total thickness (Table III; Fig. 2).

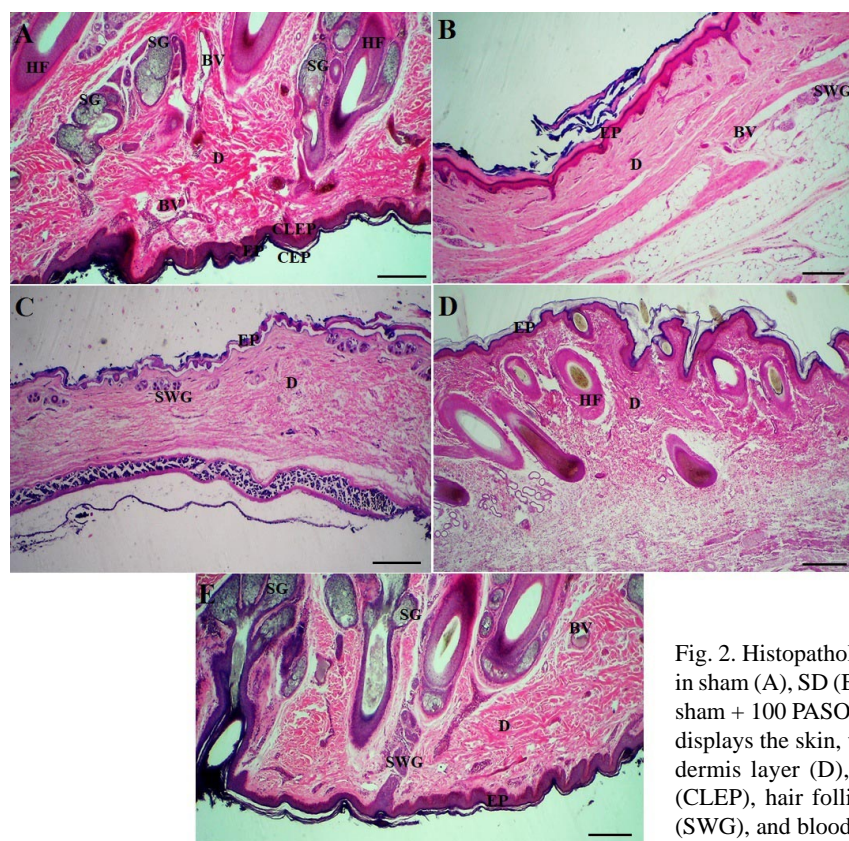


Fig. 2. Histopathology of the skin (H&E, Y10; Scale bar: 400  $\mu\text{m}$ ) in sham (A), SD (B), SD + 50 PASO (C), SD + 100 PASO (D), and sham + 100 PASO (E). The accompanying light photomicrograph displays the skin, with labels indicating the epidermis layer (EP), dermis layer (D), corneal epidermis (CEP), cellular epidermis (CLEP), hair follicle (HF), sebaceous gland (SG), sweat gland (SWG), and blood vessels (BV).

Tabla III. Thickness measurements of skin layers (in  $\mu\text{m}$ ).

Groups	Epidermal thickness			
	Cellular	Corneal	Dermal thickness	Total thickness
Sham	21.3 $\pm$ 1.6	2.9 $\pm$ 0.2	411 $\pm$ 21.1	423.1 $\pm$ 21.3
SD	8.2 $\pm$ 1.2 <sup>a</sup>	11.1 $\pm$ 0.9 <sup>a</sup>	191.1 $\pm$ 11.2 <sup>a</sup>	211.2 $\pm$ 18.4 <sup>a</sup>
Sham + 100 PASO	34.6 $\pm$ 0.9	3.3 $\pm$ 0.2	444.2 $\pm$ 21.1	461.6 $\pm$ 12.9
SD + 50 PASO	12.6 $\pm$ 1.1 <sup>b</sup>	6.2 $\pm$ 0.4	191.4 $\pm$ 15.2	261.1 $\pm$ 11.2
SD + 100 PASO	20.6 $\pm$ 2.2	3.4 $\pm$ 0.9 <sup>b</sup>	361.2 $\pm$ 16.1 <sup>b</sup>	349.7 $\pm$ 16.1 <sup>b</sup>

Data are presented as mean  $\pm$  standard deviation (SD). <sup>a</sup> $p < 0.05$  indicates a significant difference between the sham and SD groups; <sup>b</sup> $p < 0.05$  indicates significant differences among the SD + 50 PASO and SD + 100 PASO groups compared to the SD groups (one-way ANOVA with Tukey's post-hoc test).

### Role of PASO and SD on skin thiol, FRAP, and TBARS levels

The results indicate that the SD group exhibited significantly reduced levels of thiols (0.94 mmol/mg) and FRAP (1.22 mmol/mg) compared to the Sham group ( $p<0.05$ ). In contrast, the administration of 50 PASO resulted in a notable increase in thiol levels (1.15 mmol/mg) and FRAP (3.11 mmol/mg) when compared to the SD group ( $p<0.05$ ). Furthermore, the SD + 100 PASO group demonstrated a significant improvement in thiols (3.29 mmol/mg) and FRAP (6.23 mmol/mg), both substantially higher than those observed in the SD group ( $p<0.05$ ). Additionally, TBARS concentration was significantly lower in the SD + 100 PASO group (0.16 nmol/mg) compared to the SD group ( $p<0.05$ ), indicating a decrease in lipid peroxidation (LPO) (Fig. 3).

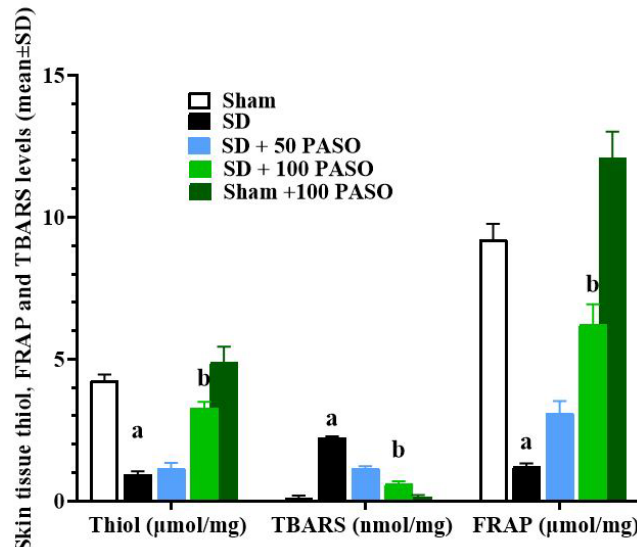


Fig. 3. Skin tissue levels of thiobarbituric acid-reactive substances (TBARS, nmol/mg; lipid peroxidation marker), ferric reducing antioxidant power (FRAP,  $\mu\text{mol}/\text{mg}$ ; antioxidant capacity), and thiol ( $\mu\text{mol}/\text{mg}$ ) across experimental groups. Data are presented as mean  $\pm$  standard deviation ( $n = 10/\text{group}$ ). <sup>a</sup> $p < 0.05$  indicates a significant difference between the sham and SD groups; <sup>b</sup> $p < 0.05$  indicates significant differences among the SD + 50 PASO and SD + 100 PASO groups compared to the SD groups (one-way ANOVA with Tukey's *post-hoc* test).

### Role of PASO and SD in regulating skin TNF- $\alpha$ , IL-1 $\beta$ , MMP-9, IL-10, MMP-2, CCR-5, and VEGF genes expression

The expression levels of regulatory and pro-inflammatory cytokines, as well as matrix metalloproteinases (MMPs) and growth factors, were significantly altered across the groups. The SD group exhibited markedly elevated levels

of IL-1 $\beta$  (5.16), CCR-5 (4.11), and TNF- $\alpha$  (4.29) compared to the Sham group ( $p < 0.05$ ). However, treatment with 50 PASO and 100 PASO resulted in significant reductions in these inflammatory markers. Notably, the SD + 100 PASO group showed a substantial decrease in IL-1 $\beta$  (1.22), CCR-5 (1.42), and TNF- $\alpha$  (1.42), indicating a positive response to the treatment ( $p < 0.05$ ). Additionally, MMP-9 and MMP-2 expression levels were significantly lower in the SD + 100 PASO group (1.23 and 1.41, respectively) compared to the SD group ( $p < 0.05$ ). In contrast, IL-10 concentrations were significantly enhanced in the SD + 100 PASO group (1.06) *versus* the SD group (0.22), indicating the treatment's anti-inflammatory impact. Furthermore, VEGF levels increased markedly in the SD + 100 PASO group (0.72) compared to the SD group (0.19), suggesting enhanced angiogenesis (Fig. 4).

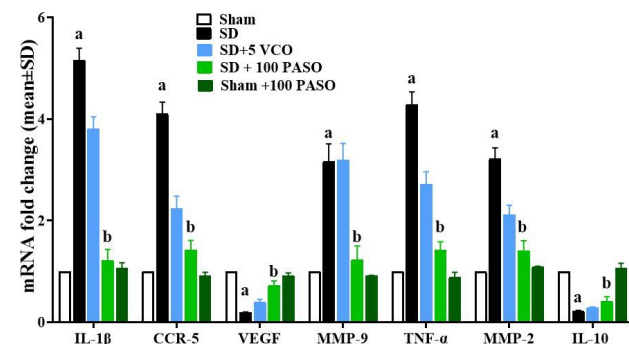


Fig. 4. Gene expression levels of pro-inflammatory cytokines IL-1 $\beta$  and TNF- $\alpha$ , anti-inflammatory cytokine IL-10, matrix metalloproteinases MMP-9 and MMP-2, chemokine receptor CCR-5, and angiogenic factor VEGF in skin tissue across experimental groups. Data represent mean  $\pm$  standard deviation ( $n = 10/\text{group}$ ). <sup>a</sup> $p < 0.05$  indicates a significant difference between the sham and SD groups; <sup>b</sup> $p < 0.05$  indicates significant differences among the SD + 50 PASO and SD + 100 PASO groups compared to the SD groups (one-way ANOVA with Tukey's *post-hoc* test).

### Role of PASO and SD in regulating skin CCR-5, MMP-2, MMP-9, and VEGF protein expression

The expression levels related to key proteins associated with inflammation and tissue remodeling were significantly altered across the experimental groups. The SD group exhibited elevated levels of CCR-5 (2.51), MMP-9 (4.29), and MMP-2 (4.21) compared to the Sham group ( $p < 0.05$ ). Treatment with 50 PASO and 100 PASO resulted in significant reductions in these markers. Notably, the SD + 100 PASO group demonstrated a marked decrease in CCR-5 (1.21) and MMP-9 (1.45), indicating a reduction in inflammatory signaling pathways ( $p < 0.05$ ). Additionally, MMP-2 concentrations were significantly lower in the SD + 100 PASO group (0.91) compared to the SD group

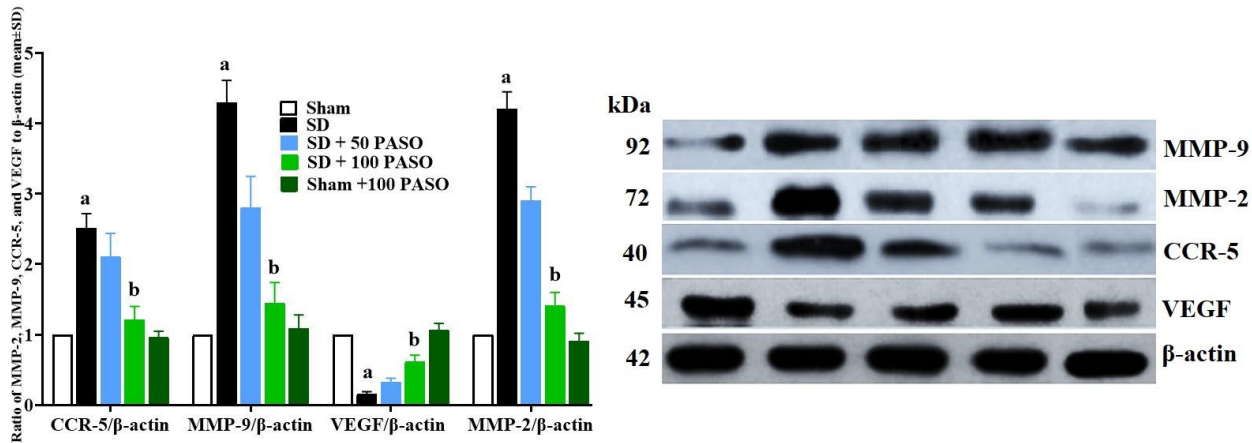


Fig. 5. Proteins expression levels of MMP-9, MMP-2, CCR-5, and VEGF (means  $\pm$  SD; n=10/group) in sham (A), SD (B), SD + 50 PASO (C), SD + 100 PASO (D), and sham + 100 PASO (E). a  $p < 0.05$  indicates a significant difference between the sham and SD groups; b  $p < 0.05$  indicates significant differences among the SD + 50 PASO and SD + 100 PASO groups compared to the SD groups (one-way ANOVA with Tukey's post-hoc test).

(4.21), further supporting the anti-inflammatory effects of the treatment. Furthermore, VEGF expression significantly increased in the SD + 100 PASO group (1.07) in comparison to the SD group (0.16), suggesting enhanced angiogenic activity in response to the treatment (Fig. 5).

## DISCUSSION

Seborrheic dermatitis (SD) is a chronic inflammatory skin disorder that predominantly affects areas rich in sebaceous glands, including the scalp, face, and chest. This condition is estimated to impact approximately 3-10 % of the global population, with a higher prevalence observed in males and individuals with compromised immune systems or neurological disorders (Honnavar *et al.*, 2024). The pathogenesis of SD is multifactorial, involving genetic predisposition, hormonal fluctuations, and environmental triggers, particularly the presence of *Malassezia* yeasts. These lipophilic fungi metabolize skin lipids, leading to an inflammatory response that is exacerbated by an imbalance between pro-inflammatory and anti-inflammatory cytokines (Piacentini *et al.*, 2025). Recent studies have highlighted the critical role of these cytokines, particularly IL-17 and IL-23, in the inflammatory cascade associated with SD. Moreover, the compromised skin barrier in SD patients increases susceptibility to irritants and pathogens, further aggravating the condition (Ghoreschi *et al.*, 2021). Given these complexities, novel therapeutic strategies focusing on specific cytokine modulation and skin microbiota restoration are being explored, including the use of probiotics and prebiotics (Dityen *et al.*, 2022). The epidemiological patterns of SD reveal peak incidences during infancy and adolescence, periods marked by significant hormonal

changes and increased sebaceous gland activity. These fluctuations often lead to the persistence of SD into adulthood, where it becomes a recurrent issue, frequently worsened by stressors (Zengin *et al.*, 2024). The male predominance in SD cases is believed to be linked to androgen-induced stimulation of sebaceous glands. Additionally, associations with neurological conditions, such as Parkinson's disease, underscore the intricate relationship between immune function and the pathogenesis of SD (Li *et al.*, 2025). Understanding these epidemiological trends is crucial for developing targeted prevention and treatment strategies that consider the unique risk factors associated with different populations.

Recent findings emphasize the role of oxidative stress in SD, where an imbalance favoring reactive oxygen species (ROS) leads to cellular damage and inflammation. Elevated levels of malondialdehyde and decreased antioxidant defenses, such as superoxide dismutase and catalase, contribute to the inflammatory milieu (Sarac *et al.*, 2022). This oxidative stress activates transcription factors like NF- $\kappa$ B, driving pro-inflammatory cytokine production and perpetuating inflammation. The interplay between these factors creates a vicious cycle that sustains the inflammatory response and exacerbates skin damage. Cytokines such as IL-6, IL-1 $\beta$ , and TNF- $\alpha$  are integral to the inflammatory response in SD. Elevated levels of IL-6 and TNF- $\alpha$  are associated with increased keratinocyte proliferation and inflammation, while IL-1 $\beta$  plays a role in immune cell recruitment and skin scaling (Li *et al.*, 2025). Conversely, the anti-inflammatory cytokine IL-10 is often diminished in affected skin, impairing the resolution of inflammation. Our study demonstrated significant alterations in oxidative stress

markers and cytokine profiles in SD, with decreased total antioxidant capacity and increased lipid peroxidation, which contribute to cellular damage and heightened inflammation (Nasser & Fonseca, 2023). The upregulation of matrix metalloproteinases (MMP-2 and MMP-9) facilitates tissue remodeling and compromises the skin barrier, while increased CCR-5 expression promotes immune cell infiltration, further sustaining the inflammatory state (Sowell *et al.*, 2022). The elevated levels of VEGF in SD lesions suggest a link to increased angiogenesis and skin hypervascularity, complicating the inflammatory landscape (Li *et al.*, 2025). Collectively, these findings highlight the multifaceted nature of SD pathogenesis, revealing potential targets for therapeutic intervention aimed at restoring balance to inflammatory processes.

PASO, derived from the kernels of the *Prunus armeniaca*, has garnered attention for its diverse pharmacological properties, including anti-inflammatory and antioxidant effects. The extraction process retains bioactive compounds that contribute to its therapeutic potential, including medium-chain fatty acids and polyphenols (Alajil *et al.*, 2021). Our study aimed to investigate the antiseborrheic effects of PASO in an animal model of SD, focusing on its influence on inflammatory and antioxidant pathways. The results indicate that PASO effectively suppressed inflammatory cytokines and inhibited MMP activity, thereby preserving the structural integrity of skin layers affected by SD. This aligns with previous research demonstrating that PASO can ameliorate oxidative stress and inflammation in various models (Cirillo *et al.*, 2023). Specifically, PASO reduced the expression of pro-inflammatory cytokines such as IL-6, IL-1 $\beta$ , and TNF- $\alpha$ , while increasing the levels of IL-10, thereby promoting an anti-inflammatory environment. Additionally, PASO enhanced the total antioxidant capacity and decreased lipid peroxidation, further supporting its role in mitigating oxidative stress associated with SD. In conclusion, the findings from this study underscore the potential of PASO as a therapeutic agent for managing seborrheic dermatitis. By targeting key inflammatory pathways and enhancing antioxidant defenses, PASO may offer a complementary approach to existing treatments. Future research should focus on clinical trials to validate these effects in human subjects and explore the underlying mechanisms of action. Furthermore, investigating the long-term efficacy and safety of PASO in diverse populations will be crucial for establishing its role in the management of SD and potentially other inflammatory skin conditions. As our understanding of the pathophysiology of SD continues to evolve, the integration of natural products like PASO into therapeutic regimens may provide a more holistic approach to skin health and wellness.

## CONCLUSION

In summary, this study demonstrates the significant potential of PASO as a therapeutic agent for managing SD. By assessing its impact on inflammatory cytokines and oxidative stress indicators in an animal model, we found that PASO effectively reduced sebum production and inflammation, which are critical factors in the pathogenesis of SD. The results highlighted that PASO treatment resulted in a marked decrease in pro-inflammatory cytokines such as IL-1 $\beta$ , and TNF- $\alpha$ , while enhancing levels of the anti-inflammatory cytokine IL-10. Additionally, the restoration of antioxidant capacity and reduction in lipid peroxidation were pivotal in mitigating oxidative stress associated with SD. Histopathological examinations confirmed the structural integrity of skin layers' post-treatment, indicating that PASO not only addresses the inflammatory aspect of SD but also promotes healing and regeneration of the skin barrier. These findings support the hypothesis that PASO can serve as an effective natural remedy for SD, offering a complementary approach to conventional therapies. Given the increasing interest in natural products for skin health, future research should focus on clinical trials to validate these findings in human subjects. Moreover, exploring the long-term efficacy and safety of PASO will be essential for its potential integration into treatment regimens for SD and other inflammatory skin conditions. Ultimately, PASO represents a promising candidate for enhancing skin health and managing chronic inflammatory disorders, paving the way for more holistic approaches in dermatological care.

**Ethical Approval.** The experimental protocols of this study were approved by Daxing Hospital, Xi'an City, Shaanxi Province ethics committee.

---

REN, N. & TAN, R. Explorando el potencial del aceite de semilla de *Prunus armeniaca* L. para la dermatitis seborreica: Un estudio estereológico, bioquímico y molecular sobre las vías de MMP-9, MMP-2, CCR-5 y VEGF en un modelo de rata. *Int. J. Morphol.*, 43(6):2070-2078, 2025.

**RESUMEN:** El aceite de semilla de *Prunus armeniaca* L. (PASO) se ha utilizado históricamente por sus beneficios medicinales, incluyendo el aumento de la vitalidad y el control del sangrado. Sus aplicaciones tradicionales están respaldadas por sus propiedades antibacterianas, antiinflamatorias y antiseborreicas. Este estudio tuvo como objetivo explorar los mecanismos que subyacen a los efectos antiinflamatorios y antiseborreicos del PASO, particularmente en relación con el recrecimiento capilar y la dermatitis seborreica (DS), mediante la evaluación de su capacidad para reducir la producción de sebo y prevenir la caída del cabello. La investigación involucró a 50 ratas Wistar, divididas en cinco grupos (n=10 cada uno): un grupo simulado, un grupo expuesto a 0.8 % de dinitrofluorobenceno (DNFB) a 2 mg/kg, dos grupos DNFB tratados con 50 y 100 mg/kg de PASO, y un grupo simulado

tratado con 100 mg/kg de paso. Al concluir el estudio, evaluamos el tejido cutáneo para determinar los niveles de citocinas inflamatorias críticas (il-1 $\beta$ , il-10 y tnf- $\alpha$ ) e indicadores de estrés oxidativo, incluyendo la capacidad antioxidante total y la peroxidación lipídica. Además, evaluamos la expresión de genes y proteínas como mmp-9, mmp-2, ccr-5 y VEGF en el tejido cutáneo. Nuestros resultados indicaron que el tratamiento con DNFB produjo cambios significativos en los niveles de antioxidantes, marcadores inflamatorios y la expresión de genes y proteínas asociados con la DS. El tratamiento con paso demostró una mejoría dependiente de la dosis, particularmente a 10 mg/kg, revirtiendo eficazmente estas alteraciones. Los análisis histopatológicos y moleculares confirmaron la restauración estructural del tejido cutáneo tras el tratamiento con PASO. En conclusión, este estudio subraya el potencial de PASO para aliviar los síntomas de la dermatitis seborreica y regular la inflamación cutánea, lo que sugiere su posible aplicación en el tratamiento de la dermatitis seborreica inducida por DNFB.

**PALABRAS CLAVE:** Aceite de coco virgen; Inflamación; Apoptosis; Antiseborreico.

## REFERENCES

Alajil, O.; Sagar, V. R.; Kaur, C.; Rudra, S. G.; Sharma, R. R.; Kaushik, R.; Verma, M. K.; Tomar, M.; Kumar, M. & Mekhemar, M. Nutritional and phytochemical traits of apricots (*Prunus armeniaca* L.) for application in nutraceutical and health industry. *Foods*, 10(6):1344, 2021.

Aleksanyan, A.; Fayvush, G.; Al Tawaha, A. R.; Al-Tawaha, A. R.; Rasyid, I.; Rahim, L. & Tenriawaru, A. N. Adaptation of *Prunus armeniaca* L. to climate change: A review. *AIP Conf. Proc.*, 3098(1):040036, 2024.

Amirouche, A.; Ait-Ali, D.; Nouri, H.; Boudrahme-Hannou, L.; Tliba, S.; Ghidouche, A. & Bitam, I. TRIzol-based RNA extraction for detection protocol for SARS-CoV-2 of coronavirus disease 2019. *New Microbes New Infect.*, 41:100874, 2021.

Bawoodood, A. S.; Afzal, M.; Tanko, A. I.; Al-Abbas, F. A.; Zeyadi, M.; Alqurashi, M. M.; Sheikh, R. A.; Alzarea, S. I.; Sayyed, N. & Kazmi, I. Malvidin improves ethanol-induced memory impairment by targeting cholinesterase, FRAP, and GABA signaling: based on molecular docking study. *J. Biol. Regul. Homeost. Agents*, 38(3):2165-79, 2024.

Cirillo, A.; De Luca, L.; Izzo, L.; Cepparulo, M.; Graziani, G.; Ritieni, A.; Romano, R. & Di Vaio, C. Biochemical and nutraceutical characterization of different accessions of the apricot (*Prunus armeniaca* L.). *Horticulturae*, 9(5):546, 2023.

Dityen, K.; Soonthornchai, W.; Kueanjinda, P.; Kullapanich, C.; Tunsakul, N.; Somboonna, N. & Wongpiyabovorn, J. Analysis of cutaneous bacterial microbiota of Thai patients with seborrheic dermatitis. *Exp. Dermatol.*, 31(12):1949-55, 2022.

Ertekin, F. & Keçeci, T. The effect of capsaicin on TBARS and TAS in rats with hypothyroidism. *J. Istanbul Vet. Sci.*, 6(2):98-104, 2022.

Fernández, J.; Jiménez, C.; Benadof, D.; Morales, P.; Astorga, J.; Cáceres, F.; Hernández, M.; Fernández, A. & Valenzuela, F. MMP-9 levels in the gingival crevicular fluid of Chilean rosacea patients. *Int. J. Mol. Sci.*, 23(17):9858, 2022.

Ghoreschi, K.; Balato, A.; Enerbäck, C. & Sabat, R. Therapeutics targeting the IL-23 and IL-17 pathway in psoriasis. *Lancet*, 397(10275):754-66, 2021.

Hill, J.; Brokamp, G. & Mosser-Goldfarb, J. Seborrheic dermatitis: from adolescence to adulthood. *Pediatr. Ann.*, 54(6):e203-e208, 2025.

Honnavar, P.; Chakrabarti, A.; Joseph, J.; Thakur, S.; Dogra, S.; Lakshmi, P. V. M. & Rudramurthy, S. M. Molecular epidemiology of seborrheic dermatitis/dandruff associated *Malassezia* species from northern India. *Med. Mycol.*, 62(10):myae104, 2024.

Jackson, J. M.; Alexis, A.; Zirwas, M. & Taylor, S. Unmet needs for patients with seborrheic dermatitis. *J. Am. Acad. Dermatol.*, 90(3):597-604, 2024.

Kassassir, H.; Papiewska-Paja, k, I.; Kryczka, J.; Boncela, J. & Kowalska, M. A. Platelet-derived microparticles stimulate the invasiveness of colorectal cancer cells via the p38MAPK-MMP-2/MMP-9 axis. *Cell Commun. Signal.*, 21(1):51, 2023.

Kapoor, R.; Shome, D.; Doshi, K.; Patel, G.; Tandel, H. & Kumar, V. A newer approach in the treatment of seborrheic dermatitis with QR678® and QR678 Neo®-A prospective pilot study. *J. Cosmet. Dermatol.*, 22(11):3078-87, 2023.

Li, J.; Feng, Y.; Liu, C.; Yang, Z.; de Hoog, S.; Qu, Y.; Chen, B.; Li, D.; Xiong, H. & Shi, D. Presence of *Malassezia* hyphae is correlated with pathogenesis of seborrheic dermatitis. *Microbiol. Spectrum*, 10(1):e0116921, 2022.

Li, Y.; Liu, Y.; Wang, S. & Li, W. Exploring the anti-seborrheic dermatitis effects of apricot kernel oil using the rat-dinitrofluorobenzene induced model: An investigation using biochemical, molecular, and histopathological methods. *Int. J. Morphol.*, 43(2):564-73, 2025.

Nasser, R. & Fonseca, A. P. Seborrheic dermatitis: exploring the pathogenesis, clinical features, and treatment strategies. *Arch. Pharm. Pharmacol. Res.*, 3(5):1-7, 2023.

Piacentini, F.; Camera, E.; Di Nardo, A. & Dell'Anna, M. L. Seborrheic dermatitis: exploring the complex interplay with *Malassezia*. *Int. J. Mol. Sci.*, 26(6):2650, 2025.

Polaskey, M. T.; Chang, C. H.; Daftary, K.; Fakhraie, S.; Miller, C. H. & Chovatiya, R. The global prevalence of seborrheic dermatitis: a systematic review and meta-analysis. *JAMA Dermatol.*, 160(8):846-55, 2024.

Sarac, G. A.; Oztekin, A.; Savci, U.; Senel, E.; Oztekin, C.; Kader, S.; Akdag, T.; Iu, S. & Erel, O. The utility of ischemia modified albumin as an oxidative stress biomarker in seborrheic dermatitis. *Ann. Med. Res.*, 29(3):290, 2022.

Sowell, J.; Pena, S. M. & Elewski, B. E. Seborrheic dermatitis in older adults: pathogenesis and treatment options. *Drugs Aging*, 39(5):315-21, 2022.

Wan, H. LB1736 Changes and their significance of Th1, Th2, Th17 cells and SCCA levels in peripheral blood of elderly patients with atopic dermatitis. *J. Investig. Dermatol.*, 143(9):B23, 2023.

Wang, T.; Chen, K.; Zhang, X.; Yu, Y.; Yu, D.; Jiang, L. & Wang, L. Effect of ultrasound on the preparation of soy protein isolate-maltodextrin embedded hemp seed oil microcapsules and the establishment of oxidation kinetics models. *Ultrasound Sonochem.*, 77:105700, 2021.

Zengin, S.; Guthrie, J.; Zoumberos, N.; Hamza, M. & Shalin, S. C. Sebaceous gland atrophy due to seborrheic dermatitis in a patient with alopecia: A potential pitfall. *J. Cutaneous Pathol.*, 51(7):513-7, 2024.

Xian, Q.; Zhou, J.; Li, X.; Xu, Y. & Sun, Y. Role of immune cells in seborrheic dermatitis: a two-sample bidirectional Mendelian randomization study. *Arch. Dermatol. Res.*, 317(1):482, 2025.

### Corresponding author:

Dr. Rongrong Tan

Department of Dermatology and Plastic Cosmetic Surgery

Daxing Hospital

Xi'an City

Shaanxi Province 710003

CHINA

E-mail: tanrong3986@outlook.com.

ORCID ID: <https://orcid.org/0009-0003-2342-4383>